Investigating the mechanical and rheological properties of 3D-printed PLA-agave biocomposites

Ferenc Palásti
John von Neumann University
Pál Hansághy
John von Neumann University
Péter Gerse
John von Neumann University
Erika Varga
John von Neumann University
Kanageswary Sockalingam
Asia Pacific University of Technology & Innovation
Chan Mieow Kee
SEGi University
László Tóth
toth.laszlo@nje.hu
John von Neumann University

Research Article

Keywords: recycling, PLA, biocomposites, Agave Americana, 3D printing

Posted Date: July 14th, 2026

DOI: https://doi.org/10.21203/rs.3.rs-9978775/v1

Additional Declarations: No competing interests reported.

Abstract

The increasing generation of polylactic acid (PLA) based 3D printing wastes has driven the need for sustainable strategies to improve properties of recycled materials. This study focuses on the effect of low natural fiber concentration in enhancing mechanical and rheological properties of recycled PLA (rPLA). Agave Americana fibers at 1, 2, and 3 wt.% were used as reinforcement for the PLA-based bio-composite films. The composites were fabricated via extrusion and mechanical properties such as tensile, impact, and flexural were analysed. Melt flow rate (MFR), Fourier Transform Infrared Spectroscopy (FTIR) and Scanning Electron Microscope (SEM) were used to understand the samples behaviour. Results obtained demonstrated significant recovery in mechanical properties for composites at 1 wt.% fiber loadings. Increasing fiber content up to 3 wt.% led to decline in tensile and flexural properties due to poor interfacial bonding and void formation, as confirmed by SEM observations. FTIR analysis show the presence of hydroxyl groups in agave fiber and its bio-composites, indicating weak fiber-matrix adhesion. This was further supported by MFR values that increased with the addition of fibers, resulting in lower viscosity. This was directly attributed to enhanced flowability induced from PLA chain scission and shear thinning behaviour.

1. Introduction

Additive manufacturing, also known as 3D printing, is a transformative technology that constructs three-dimensional objects by adding material layer by layer, based on a Computer Aided Design (CAD) model. Unlike traditional manufacturing methods, 3D printing allows rapid fabrication of complex structures and highly customized products, tailored to specific needs and preferences [1, 2]. Since its commercialization in the 21st century, 3D printing has seen significant growth in both application and technological advancement, making it a versatile tool across various industries such as agricultural, medical, automotive, aerospace, engineering, and consumer goods [3, 4].

Fused Deposition Modelling (FDM), is a 3D printing method, widely used in printing polymer-based materials such as polylactic acid (PLA) [5, 6]. PLA is one of the most extensively utilized materials in FDM due to its excellent printability, and on top of all that favourable biodegradability and sustainability position it among the most desirable raw materials. Produced from renewable resources such as sugarcane and cornstarch, PLA has increasingly replaced many conventional polymers derived from fossil fuels. In recent years, PLA production has been increasing rapidly and is expected to exceed 2.4 million metric tons by 2027 [7].

Despite its advantages, 3D printing waste generated from PLA has been increasing rapidly. Common forms of waste include discarded prints, support structures, and failed iterations, many of which are ultimately landfilled [8]. The degradation of PLA in landfill environments is generally slower and less efficient than in composting systems due to the absence of optimal conditions such as elevated temperatures and adequate oxygen availability [9]. A study by Agwuncha et al. [10] reported that under

real-world landfill conditions, no changes or degradation was observed for pristine PLA even after 13-week (91 days) burial period.

Therefore, recycling plays a crucial role in mitigating waste generated from PLA-based 3D printing. Recycling not only reduces landfill accumulation but also minimize dependence on pristine raw materials, thereby contributing to a more sustainable manufacturing cycle. This approach aligns with the circular economy model, which promotes the continuous use and reuse of materials across multiple stages and life cycles rather than disposal after a single use [11]. Over the past decades, researchers have actively explored the potential of recycling PLA filaments as a strategy to reduce plastic waste. For instance, Oladapo et al. [12] examined the possibility of achieving net-zero waste in additive manufacturing, finding that producing recycled filament consumes less energy than creating pristine PLA, which results in lower greenhouse gas emissions.

However, the primary limitation of recycled PLA (rPLA) compared to pristine PLA (oPLA) is its reduced mechanical properties. This includes lower tensile strength, fatigue strength, and hardness, which are critical for the structural integrity of 3D printed parts [7]. While rPLA can serve as an alternative to pristine PLA, its properties require appropriate modification and control through methods such as blending with pristine materials, reinforcing with natural fibers [13], altering printing parameters, and using additives to enhance its performance. Incorporating natural fibers into recycled polylactic acid (PLA) can significantly enhance its mechanical, rheological and thermal properties, making it a more viable material for various applications, including additive manufacturing [14–18].

Faidallah et al. [19] reported that rPLA reinforced with 7 wt.% hemp fibers achieved a tensile strength of 38.8 MPa, which is a 29% increase over pristine PLA filaments and a 26% improvement compared to rPLA without reinforcement. Wang et al. [20] incorporated abutilon fibers with PLA, that resulted in improved thermal stability and crystallization of PLA. This was linked to natural fibers acting as nucleating agents, enhancing the crystallization and thermal stability of PLA. The use of natural fibers like cocoa pod husk and dragon fruit root not only improved the mechanical properties but also enhanced the biodegradation rate of PLA biocomposites, demonstrating a 6.4% weight loss in soil within 15 days [21].

Among many fibers reported, agave fibers are one of the less explored reinforcement in PLA for 3D printing filaments [22]. Agave americana is a succulent plant from the Agavaceae family, native to Central America and Mexico. It has been successfully introduced and extensively cultivated in tropical and subtropical regions worldwide, and capable of achieving yields exceeding 300 tons per hectare per year [23, 24]. The fibers from this plant are commonly used in rope making and textile production. However, only approximately 4 wt.% of the harvested leaves is converted into commercially valuable products. Agave fibers primarily consist of cellulose (68.4%), followed by hemicellulose (15.7%) and lignin (4.9%), with the remaining 11.06% comprising fructans, pectins, and other simple carbohydrates [23].

Hence, this study aims to investigate the potential of agave fibers as a sustainable reinforcement to enhance the properties of rPLA. agave fibers will be utilised as reinforcement to enhance the mechanical and physical performance of rPLA for FDM applications. The influence of different fiber loadings will be systematically examined to determine their effects on the composite behaviour and filament quality. The developed rPLA–agave biocomposite filaments are expected to provide a more sustainable and biodegradable alternative for 3D printing materials while simultaneously valorising agricultural waste.

2. Materials and Methods

2.1. Raw Materials Preparation

The agave fibers (AF) were derived from the *Agave Americana* plant. The plant was cut and peeled, then dried for one week at 60°C. Waste materials were removed using distilled water, after which the fibers were dried for four hours at 80°C. Finally, the dried fibers were milled in a labratory ball mill until the desired fraction below 250 µm was obtained. The PLA used in this study was an iPLA type (with MFR: 24.7 g/10 min, 2.16 kg, 210°C), specifically designed for 3D printing. Recycled PLA was obtained by reprocessing the extruded pristine PLA filaments using the same equipment and parameters as during the filament preparation.

2.2. Filament Fabrication

Prior to extrusion, pristine PLA and rPLA was dried at 60°C for 24 hours, while agave was dried at 70°C for 72 hours. The rPLA/agave composites were produced using a Labtech 26–44 (Labtech Engineering, Thailand) type 26 mm screw diameter twin screw extruder with an L/D ratio of 48, zone temperatures between 180–210°C and a screw speed of 10 rpm. AF content was kept at 1, 2, and 3 wt.% and particular attention was given to ensure uniform dispersion of the fibers throughout the PLA matrix. The composite blends were subjected to air cooling and subsequently fed into a granulator, where they were pelletized into cylindrical-shaped granules. The granules were then melted and pushed through the filament extruder, producing filaments with specified diameter of 1.75 mm.

2.3 FDM Printing

The specimens were printed on an open work area Craftbot Plus (Craftbot Hungary) 3D printer. The printer has an all-metal hot end and the tray is covered with Kapton film. The GCODE for the 3D printer was created using the Craftware slicer software version 1.23 released by Craftbot. The specimens were printed with a temperature head of 215°C and a table temperature of 60°C. The nozzle is made of 0.4 mm in diameter copper and the layer thickness is 0.2 mm, with a printing speed of 60 mm/s. Samples were printed in three different dimensions to suit tensile, bending and impact test standard. The test specimen is composed of a total of 20 layers, arranged perpendicular to each other at 45° and − 45°. Pristine PLA and rPLA specimens without reinforcement were printed as control sample and marked as oPLA and rPLA-A0, respectively. Composites containing 1, 2, and 3 wt.% agave fibers were printed and designated as rPLA-A1, rPLA-A2, and rPLA-A3, respectively.

2.4 Mechanical Testing

Tensile, flexural and Charpy impact tests were carried out on the 3D printed specimens in according to MSZ EN ISO 527, MSZ EN ISO 178, and MSZ EN ISO 179, respectively. Tensile properties, including modulus of elasticity, tensile strength, and elongation at break, were determined using an Instron 3366 universal testing machine (Instron Inc., Norwood, MA, USA) at a crosshead speed of 300 mm/min and a gauge length of 100 mm. The same testing machine was used for the three-point bending tests, conducted with a support span of 64 mm and a test speed of 20 mm/min. The Charpy impact tests were performed using a Ceast Impactor II impact tester (Instron Inc., Norwood, MA, USA) equipped with a 5 J pendulum, with the support span set at 64 mm. All mechanical tests were carried out under standard laboratory conditions, and at least five specimens were tested for each condition to ensure accuracy.

2.5 Scanning Electron Microscopy (SEM)

The surface morphology of the 3D printed samples was investigated using Scanning Electron Microscopy (SEM). SEM was conducted using a Zeiss Sigma 300 VP equipped with a secondary electron (SE) detector. The measurements were performed at an accelerating voltage of approximately 1 kV, eliminating the need for a conductive coating on the samples. This approach provides more accurate particle dimension measurements. Broken test pieces from Charpy impact test were used for this investigation.

2.6 Fourier Transform Infrared Spectroscopy (FTIR)

The chemical structure of all the samples was analyzed by Fourier Transform Infrared Spectroscopy (FTIR) with attenuated total reflectance (ATR) diamond accessory. The spectra were obtained using 64 scans at a spectral resolution of 4 cm^{-1} over the wavenumber range of 4000–500 cm^{-1}

2.7 Melt Flow Rate (MFR) Testing

The flow behaviour and processability of the created PLA/agave composites were studies via Melt Flow Rate (MFR) analysis. The test was performed with a Ceast MF10 device, at 210°C temperature with 2.16 kg standard applied load. Results were recorded in g/10 min.

3. Results and Discussion

3.1 Mechanical Properties of rPLA/agave Composites

3.1.1 Tensile Strength Analysis

Tensile properties of oPLA and rPLA samples are presented in Fig. 1. A reduction of approximately 38.9% in tensile strength was observed after extrusion, with values decrease from 62.8 MPa for oPLA to 38.4 MPa for rPLA-A0. The modulus of elasticity also reduced from 2791 MPa (oPLA) to 1911 MPa (rPLA-A0). This can be attributed to the increase in the crystallinity of PLA due to recycling. Recycling

often leads to reduction in molecular weight, where the polymer chains become more mobile, allowing them to rearrange into more crystalline structures [25]. This was also proved from slight reduction in elogation at break for rPLA-A0 sample as shown in Fig. 1(c). The increase in crystallinity can lead to brittleness, which reduces the elongation [26].

The addition of 1 wt.% agave fiber significantly enhanced the tensile strength of rPLA-A1 to 58.5 MPa, corresponding to an increase of approximately 52.3%. Similarly, the elastic modulus improved by about 55%. These results suggest that the mechanical performance was nearly recovered to that of the oPLA, with only a marginal difference of 6.9%. The increase in tensile strength with 1 wt.% agave fibers may be due to fibers acting as stress transfer agent improving stiffness and strength. However, further addition of agave fibers to 2 wt.% and 3 wt.% reduced the tensile strength to 43.6 MPa and 35.4 MPa, respectively. A total of 39.5% in reduction was observed with addition of agave fibers from 1 wt.% to 3 wt.%. The tensile strength of PLA composites generally increases with fiber loading up to a possible optimum point, followed by a subsequent decrease [27].

3.1.2 Impact Strength Analysis

The impact strength of pristine PLA, recycled PLA as well as agave fiber reinforced PLAs are presented in Fig. 2. Pristine PLA exhibits highest impact strength of 16.67 kJ/m², while recycling leads to a reduction of approximately 18.5%, decreasing the value to 13.59 kJ/m². The results correlates to tensile strength of the specimens that showed similar patern, where recycling leads to thermal degradation and chain scission resulting in molecular weight reduction. While tensile properties are influenced by load transfer efficiency, impact strength is governed by energy absorption mechanisms; however, both are adversely affected by processing temperatures. Similar results were reported by Chien et al. [25], who investigated the mechanical properties of 3D printed PLA-Wood fiber composites. The study reported noticeable reduction in impact strength after two times recycling. Analysis from gel permeation chromatography (GPC) revealed deterioration in molecular weight of PLA matrix and an increase in crystallinity.

Referring data presented in Fig. 2, reinforcement with 1 wt.% agave fibers shows minimal increase in impact strength with values of 13.62 kJ/m² (rPLA-A1). This represents an increase of approximately 0.2%, which is considered negligible. This suggests limited effectiveness of the fibers in enhancing energy absorption, likely due to insufficient fiber–matrix interaction and ineffective stress transfer mechanisms at low fiber content. Subsequent increase in fiber loadings (2 wt.% and 3 wt.%) showed a pronounced reduction in the impact strength to 13.17 kJ/m² (rPLA-A2) and 10.06 kJ/m² (rPLA-A3). A total reduction of about 26.1% was observed with increased fiber loadings from 1 wt.% to 3 wt.%. This indicates a decrease in toughness of the specimens, possibly due to void formation and stress concentration sites caused by poor interfacial bonding [28]. These findings are consistent with the SEM observations, where fiber pull out, interfacial gaps and voids were evident in samples with higher fiber loadings (Fig. 4).

3.1.3 Flexural test results

Flexural strength and modulus are an important measure of the load-bearing capacity and stiffness of the developed composites under bending condition. Figure 3 represents flexural strength, modulus, and deflection of the composite samples. Results obtained correlates with the tensile and impact properties reported, where recycling reduces the flexural strength and modulus up to 29.1% and 19.3%, respectively. Addition of 1 wt.% agave fiber partially recovers the flexural strength up 26.5%. The flexural strength of oPLA remains the highest with 98.85 MPa, followed by rPLA-A1 and rPLA-A2, which values at 88.61 MPa and 75.35 MPa. The observed partial recovery in strength indicates the potential of recycled PLA for 3D printing applications and suggests that 1 wt.% fiber loading as optimum condition for this composite system. A study conducted by laylamia et al. [29] reports optimal flexural strength in bio epoxy composite occurs at 30 wt.% of Agave waste flower stalk fibers addition, attributing this to uniform fiber dispersion and strong interfacial bonding. However, the enhancement in strength at low fiber loading (1 wt.%) in the present study may be linked to initial contribution of fibers to load-bearing and stiffness enhancement, instead of strong fiber-matrix adhesion.

The flexural strength and modulus of the composites samples at higher fiber loading (3 wt.%) continues to deteriote to 60.65 MPa, which is significantly lower than the recycled PLA without reinforcement (70.07 MPa). However, further increases in fiber content lead to a deterioration in mechanical performance, attributed to poor interfacial bonding, and crack formation. Another parameter worth noting is the deflection of the samples, which can be observed in Fig. 3(c). Pristine PLA indicates highest deflection (7.81 mm), which decreases upon recycling, suggesting reduction in ductility due to polymer degradation. Incorporation of agave fiber at low loadings (1 wt.%), decreases the deflection to 5.74 mm, representing the lowest value among all samples. This behaviour indicates reduction in deformability, where the fibers restricts polymer chain mobility, limiting deformation under applied load. However, the subsequent increase deflection for rPLA-A2 and rPLA-A3, may be related to the poor dispersion of the fiber that weakened internal structure, allowing greater deformation under load.

3.2 Surface morphology of rPLA/agave composites

The fracture surfaces of FDM-printed rPLA/agave fiber composites after impact testing were examined using SEM. Figures 4 illustrate the morphology of the samples at low and high magnifications. Based on Fig. 4(a), rPLA without reinforcement exhibits a brittle fracture behaviour with uniform fracture surface. The printed roads and inter-road boundaries are clearly visible indicating limited resistance to impact loading, which was also evidenced by reduced tensile, flexural and impact properties of the recycled PLA. Meanwhile, rPLA-A1 (Fig. 4(c)) exhibits increased surface roughness, where the inter-road boundaries are not visible, which can be associated with increased energy dissipation during fracture. At higher magnifications (Fig. 4(d)), although the fiber dispersion seems good, the interfacial bonding remains limited as early signs of fiber pull out seems present. This is in accordance with the mechanical tests results, where stiffness increases but impact strength shows insignificant increment.

Increasing fiber loadings to 2 wt.% (Fig. 4(f)) and 3 wt.% (Fig. 4(h)) showed changes in the microstructure where increased voids and cracks are observed within the fracture surface, that became more irregular and heterogenous. High-magnification images further revealed interfacial gaps, and enlarged pull-out cavities, indicating weakened interfacial bonding due to insufficient matrix wetting and non-uniform fiber dispersion. These defects subsequently promote stress localization and premature crack initiation, offsetting the potential benefits of increased fiber content. Similarly Ramirez et al. [30] examined the fracture surface morphology of neat PLA and its composite systems using SEM and reported observations consistent with the present findings. The incorporation of 1 wt.% sisal fibers resulted in increased surface roughness, which became more pronounced with higher fiber loadings. The SEM micrographs revealed evident fiber detachment and voids formed by fiber pull-out, indicating weak interfacial adhesion between the fibers and the PLA matrix.

3.3 Fourier Transform Infrared Spectroscopy (FTIR) analysis

FTIR spectra of raw agave fiber, pristine PLA, recycled PLA and its bio composites are shown in Fig. 5. The finding confirms presence of lignocellulosic components, namely cellulose, hemicellulose and lignin in the raw fiber. A broad absorption band at 3285 cm^{-1} is observed in the raw fiber sprectrum, which is attributed to the O–H stretching vibration of the hydroxyl group (OH) present in cellulose [31]. However, this peak is not seen in any of the biocomposite samples, likely due to decreased water content due to extrusion process [32]. Additionally, the peak at 2918 cm^{-1} in the raw fiber corresponds to C–H stretching vibration group of cellulose in the fiber. The peak at 1594 cm^{-1}, close to the 1600 cm^{-1} could be attributed to C = O stretching of the amide group in hemicellulose. A notable peak at 1027 cm^{-1} indicates C–OH stretching of lignin, similar to which had been reported by da Silva Neto et al. [23].

Meanwhile, the pristine PLA shows characteristics peaks of CH_2 stretching bands at 2998 and 2940 cm^{-1}. High intensity C = O stretching bands are also present at 1750 cm^{-1}, along with CH_2 bending bands at 1451 cm^{-1} [23]. Bands at 1178 and 1080 cm^{-1} can be associated with C-O-C bending. Peaks at 865 and 750 cm^{-1} represent the crystalline and amorphous fractions of pristine PLA, respectively [33]. The spectrum of recycled PLA (rPLA-A0) and the bio-composites showed similar peaks to pristine PLA, as depicted in Fig. 5. This may be due to the low concentrations of agave fibers used, preventing significant changes in the chemical structure of the PLA. Nevertheless, changes in the peak intensity at 1750 cm^{-1} can be noticed as the fiber concentrations increased in the bio-composites, corresponding to the fiber-matrix interaction. Similar findings were reported by Palaniappan et al. [34], who investigated the effects of incorporating peanut hull (AHL) particles into PLA for production of 3D printing filament. The study observed a decrease in the peak intensity at 1745 cm^{-1} with increasing AHL content, which was attributed to the interaction between the carbonyl groups of the PLA matrix and the hydroxyl groups of the AHL particles.

3.4 Rheological Properties of PLA/Agave Composites

MFR is a critical parameter in 3D printing as it affects material's extrudability and printability. The flow behaviour of oPLA, rPLA-A0, rPLA-A1, rPLA-A2, and rPLA-A3 blends, were analysed via MFR before printing the test pieces. Results obtained were plotted in Fig. 6. The MFR values shows increasing trend with the addition of agave fibers, which consequently indicates the reduction in viscosity. The value increases from 24.7 g/10 min for pristine PLA, up to 50.25 g/10min for composites with 2 wt.% of fibers (rPLA-A2). Slight decrement was observed in sample with 3 wt.% agave fibers, where the MFR value is at 46.9 g/10 min at 3 wt.% (rPLA–A3).

Results obtained deviates from conventional expectations, where increasing fiber concentration usually leads to increase in viscosity, mainly due to reduced flowability [35]. However, PLA based natural fiber composites doesn't always behave in a similar way, as several factors may affects its melt flowability such as moisture content of fibers and PLA chain scission induced by thermomechanical processing. This is evident from study done by Mazzanti et al. [36], who analysed effects of hemp fiber addition on stability of PLA in the molten state. The study shows increased MFR values with addition of hemp fiber and linked this with moisture trapped in the fibers that promote hydrolysis of PLA chains during thermal processing.

In the present study, FTIR spectrum of raw agave fiber (Fig. 5) showed a broad O–H peak around 3285 cm^{-1} which confirms the presence hydroxyl groups. In addition, the reduction in the peak intensity around 1750 cm^{-1} in the biocomposite spectra further suggest the interaction between hydroxyl groups of agave fiber and carbonyl groups of PLA [37]. Hydroxyl groups makes agave fibers hydrophilic and retain residual moisture even after drying process. Hence during thermal processing, these hydroxyl-bearing fibers promotes degradation of ester linkages in PLA, resulting in chain scission [38]. PLA chain scission subsequently leads to molecular weight reduction and enhances polymer chain mobility, thereby increases the MFR values (reduced viscosity).

On the other hand, the increase in MFR value may also be linked with shear thinning behaviour during melt processing [39]. Fibers in the PLA acts as stress concentrators, help aligning polymer chains under shear, thus increasing flowability. The slight reduction in MFR value at 3 wt.% fiber (rPLA-A3) is likely due to the onset of fiber agglomeration that hinder polymer chain mobility and reduce flowability. The rheological properties of the biocomposites are consistent with mechanical tests results, where only minimal increase in tensile strength were observed at low fiber loading, followed by deterioration as fiber concentration increased. This further proves that, the increase in MFR value had been caused by PLA chain scission, rather than improved fiber dispersion or processability. Overall, this characteristic is advantageous for 3D printing applications, as higher MFR value facilitates extrusion and printability of the composite samples.

4. Conclusion

This study investigates the potential to enhance properties of recycled PLA via addition of low concentration of agave fibers, while simultaneously reducing environmental impact by eliminating the use of chemical treatments. Results obtained demonstrated significant recovery of tensile strength up to 52.3% for recycled PLA with 1 wt.% of agave fiber addition. Similarly, addition of 1 wt.% agave fiber partially recovers the flexural strength up 26.5%, indicating effective stress transfer. This suggests that low fiber loading can effectively compensate performance deterioration associated with recycling. In contrast, higher fiber loading at 2 and 3 wt.%, reduces the tensile, impact and flexural properties of the composites, attributed to limited interfacial adhesion and defect formation as proved by SEM images. The poor interfacial addition was further supported by FTIR results, where absence of significant chemical interaction was observed. These findings indicate that low concentration of agave fiber offers a simple and sustainable strategy in improving properties of recycled PLA.

5. Limitation and Recommendation

This study is limited by the absence of direct molecular weight analysis. Present study primarily dependent on MFR and FTIR results to predict the molecular degradation of the bio-composites. Future work should include Gel Permeation Chromatography test to determine molecular weight characterization before and after recycling as well as composite fabrication. Although chemical treatment of fibers was intentionally avoided in this study to reduce environmental impact, future work may include surface modification as a comparative approach to evaluate its effect on composite performance.

Declarations

Funding Declaration

The corresponding author reports was provided by John von Neumann University. The other authors declare that they have no known competing financial interests or personal relationships that could have appeared to influence the work reported in this paper.

Author Contribution

Ferenc Palásti - Conceptualization, Methodology, Validation, Investigation, Resources, Writing (Original Draft), Writing (Review & Editing)Pál Hansághy - Validation, Investigation, Writing (Original Draft), Péter Gerse - Validation, Investigation, Writing (Original Draft), Erika Varga - Conceptualization, Methodology, Resources, Writing (Original Draft), Writing (Review & Editing)Kanageswary Sockalingam - Methodology, Writing (Original Draft), Chan Mieow Kee - Methodology, Writing (Original Draft), László Tóth - Conceptualization, Investigation, Writing (Original Draft), Writing (Review & Editing)

References

1. Apicella A, Scarfato P, Incarnato L (2025) Study on 3D printability of PLA/PBAT/PHBV biodegradable blends for packaging applications. Polym Test 145:108748. https://doi.org/10.1016/j.polymertesting.2025.108748
2. Beg MDH, Pickering KL, Akindoyo JO, Gauss C (2024) Recyclable hemp hurd fibre-reinforced PLA composites for 3D printing. J Mater Res Technol 33:4439–4447. https://doi.org/10.1016/j.jmrt.2024.10.082
3. Tuli NT, Khatun S, Rashid AB (2024) Unlocking the future of precision manufacturing: A comprehensive exploration of 3D printing with fiber-reinforced composites in aerospace, automotive, medical, and consumer industries. Heliyon 10:e27328. https://doi.org/10.1016/j.heliyon.2024.e27328
4. Kónya G, Ficzere P (2023) The Effect of Layer Thickness and Orientation of the Workpiece on the Micro- and Macrogeometric Properties and the Machining Time of the Part during 3D Printing. Periodica Polytech Mech Eng 67:143–150. https://doi.org/10.3311/PPme.21473
5. Zu R, Chen W, Huang Y et al (2025) Tailor-made 3D printing TPU/PLA composites for damping and energy absorption. Mater Design 252:113752. https://doi.org/10.1016/j.matdes.2025.113752
6. Ádám B, Weltsch Z (2021) Thermal and Mechanical Assessment of PLA-SEBS and PLA-SEBS-CNT Biopolymer Blends for 3D Printing. https://doi.org/10.3390/app11136218. Applied Sciences 11:
7. Hasan MR, Davies IJ, Pramanik A et al (2024) Potential of recycled PLA in 3D printing: A review. Sustainable Manuf Service Econ 3:100020. https://doi.org/10.1016/j.smse.2024.100020
8. Poddar M, Chang Y-H, Yadav M, Chiu F-C (2025) Sustainable valorization of 3D printing waste: Electrospun colored PLA nanofibers for high-performance oil adsorption and regeneration. J Environ Chem Eng 13:119557. https://doi.org/10.1016/j.jece.2025.119557
9. Hussain M, Khan SM, Shafiq M, Abbas N (2024) A review on PLA-based biodegradable materials for biomedical applications. Giant 18:100261. https://doi.org/10.1016/j.giant.2024.100261
10. Agwuncha SC, Chukwu FO, Azeh Y, Ojo K (2022) Assessment of the Degradation of PLA/PCL Biocomposites in a Landfill Environment. Nigerian Res J Eng Environ Sci 7. https://doi.org/10.5281/zenodo.6724684
11. Hidalgo-Carvajal D, Muñoz ÁH, Garrido-González JJ et al (2023) Recycled PLA for 3D Printing: A Comparison of Recycled PLA Filaments from Waste of Different Origins after Repeated Cycles of Extrusion. Polymers 15. https://doi.org/10.3390/polym15173651
12. Oladapo BI, Bowoto OK, Adebiyi VA, Ikumapayi OM (2023) Net zero on 3D printing filament recycling: A sustainable analysis. Sci Total Environ 894:165046. https://doi.org/10.1016/j.scitotenv.2023.165046
13. Punia Bangar S, Ilyas RA, Chaudhary N et al (2023) Plant-Based Natural Fibers For Food Packaging: A Green Approach To The Reinforcement of Biopolymers. J Polym Environ 31:5029–5049. https://doi.org/10.1007/s10924-023-02849-3
14. Plamadiala I, Croitoru C, Pop MA, Roata IC (2025) Enhancing Polylactic Acid (PLA) Performance: A Review of Additives in Fused Deposition Modelling (FDM) Filaments.

https://doi.org/10.3390/polym17020191. Polymers 17:

15. Muthe LP, Pickering K, Gauss C (2022) A Review of 3D/4D Printing of Poly-Lactic Acid Composites with Bio-Derived Reinforcements. Compos Part C: Open Access 8:100271. https://doi.org/10.1016/j.jcomc.2022.100271
16. Asrofi M, Hastu MOP, Anshori MLA et al (2025) The Effect of Alkalization Fiber on Mechanical, Microstructure, and Thermal Properties of Sugarcane Bagasse Fiber Reinforced PLA Biocomposite. J Renew Mater 13:1979–1992. https://doi.org/10.32604/jrm.2025.02025-0033
17. Dananjaya V, Yang M, Zheng Y, Abeykoon C (2025) Effect of filler characteristics and processing route on bamboo powder-reinforced PLA composites. J Clean Prod 537:147193. https://doi.org/10.1016/j.jclepro.2025.147193
18. Czajka-Warowna A, Sztorch B, Frydrych M et al (2026) Dual Interface Engineering in PLA: Co-equal Roles of Silanization and Chain Extension for Agri-Food Lignocellulosic Filler. J Polym Environ 34:56. https://doi.org/10.1007/s10924-026-03786-7
19. Faidallah RF, Hanon MM, Salman ND et al (2024) Development of Fiber-Reinforced Polymer Composites for Additive Manufacturing and Multi-Material Structures in Sustainable Applications. Processes 12. https://doi.org/10.3390/pr12102217
20. Wang H, Hassan EAM, Memon H et al (2019) Characterization of Natural Composites Fabricated from Abutilon-Fiber-Reinforced Poly (Lactic Acid). https://doi.org/10.3390/pr7090583. Processes 7:
21. Asrofi M, Rafid M, Pradiza RR et al (2025) Mechanical and Physical Properties of PLA Biocomposites Reinforced With Hybrid Fiber From Cocoa Pod Husk and Dragon Fruit Root for Flexible Packaging. J Vinyl Add Tech 31:975–984. https://doi.org/10.1002/vnl.70012
22. Figueroa-Velarde V, Diaz-Vidal T, Cisneros-López EO et al (2021) Mechanical and Physicochemical Properties of 3D-Printed Agave Fibers/Poly(lactic) Acid Biocomposites. Materials 14. https://doi.org/10.3390/ma14113111
23. da Silva Neto T, de Freitas JVG, Barbosa RFS et al (2023) Enhancement of sustainable fused deposition modeling 3D-printing with agave Americana fiber-reinforced poly(lactic) acid biofilaments. J Appl Polym Sci 140:e54622. https://doi.org/10.1002/app.54622
24. Hulle A, Kadole P, Katkar P (2015) Agave Americana Leaf Fibers. Fibers 3:64–75. https://doi.org/10.3390/fib3010064
25. Chien Y-C, Wu J-H, Shu C-H et al (2024) Closed-Loop Recycling of 3D-Printed Wood–PLA Composite Parts: Effects on Mechanical and Structural Properties via Fused Filament Fabrication. Polymers 16. https://doi.org/10.3390/polym16213002
26. Hocker SJA, Kim WT, Schniepp HC, Kranbuehl DE (2018) Polymer crystallinity and the ductile to brittle transition. Polymer 158:72–76. https://doi.org/10.1016/j.polymer.2018.10.031
27. kumar S, Shamprasad M, Varadarajan Y (2021) Mechanical properties of natural fiber reinforced polylactide composites: A review. IOP Conference Series: Materials Science and Engineering 1065:012001. https://doi.org/10.1088/1757-899X/1065/1/012001

28. Huerta-Cardoso O, Durazo-Cardenas I, Marchante-Rodriguez V et al (2020) Up-cycling of agave tequilana bagasse-fibres: A study on the effect of fibre-surface treatments on interfacial bonding and mechanical properties. Results Mater 8:100158. https://doi.org/10.1016/j.rinma.2020.100158
29. Lalaymia I, Belaadi A, Chai BX, Ghernaout D (2026) Structural and thermomechanical characterization of a new bio-epoxy composite reinforced with agave waste flower stalk fibers for sustainable applications. Ind Crops Prod 241:122800. https://doi.org/10.1016/j.indcrop.2026.122800
30. Ramirez C, Agaliotis E, Pettarin V (2024) Fracture toughness and overall characterization of PLA based biocomposites with natural fibers: A comparative study. Polymer 307:127309. https://doi.org/10.1016/j.polymer.2024.127309
31. Rahman MM, Reza MS, Maniruzzaman M (2026) Fabrication and characterization of biocomposites from acetylated and bleached Agave atroverance L. fibers by grafting of styrene to enhance their thermomechanical, physicochemical, and morphological properties: A new approach. S Afr J Chem Eng 55:586–604. https://doi.org/10.1016/j.sajce.2026.01.001
32. Lazaro-Romero A, Contreras-Ramos SM, Dehonor-Gómez M et al (2024) Optimizing cellulose fraction for enhanced utility: Comparative pre-treatment of Agave tequilana Weber var. blue bagasse fiber for sustainable applications. Heliyon 10:e29149. https://doi.org/10.1016/j.heliyon.2024.e29149
33. Rocca-Smith J, Lagorce-Tachon A, Iaconelli C et al (2017) How high pressure CO2 impacts PLA film properties. Express Polym Lett 11:320–333. https://doi.org/10.3144/expresspolymlett.2017.31
34. Palaniyappan S, Sivakumar NK, Dalaq AS (2026) A peanut-hull-PLA based 3D printing filament with antimicrobial effect. J Manuf Process 160:242–253. https://doi.org/10.1016/j.jmapro.2026.01.064
35. Mantia FPL, Morreale M (2011) Green composites: A brief review. Compos Part A: Appl Sci Manufac 42:579–588. https://doi.org/10.1016/j.compositesa.2011.01.017
36. Ilyas RA, Zuhri MYM, Aisyah HA et al (2022) Natural Fiber-Reinforced Polylactic Acid, Polylactic Acid Blends and Their Composites for Advanced Applications. Polymers 14. https://doi.org/10.3390/polym14010202
37. Gregor-Svetec D, Leskovšek M, Leskovar B et al (2021) Analysis of PLA Composite Filaments Reinforced with Lignin and Polymerised-Lignin-Treated NFC. https://doi.org/10.3390/polym13132174. Polymers 13:
38. Tahir M, Seyam A-F (2025) Greening Fused Deposition Modeling: A Critical Review of Plant Fiber-Reinforced PLA-Based 3D-Printed Biocomposites. https://doi.org/10.3390/fib13050064. Fibers 13:
39. Mazzanti V, de Luna MS, Pariante R et al (2020) Natural fiber-induced degradation in PLA-hemp biocomposites in the molten state. Compos Part A: Appl Sci Manufac 137:105990. https://doi.org/10.1016/j.compositesa.2020.105990

Figures

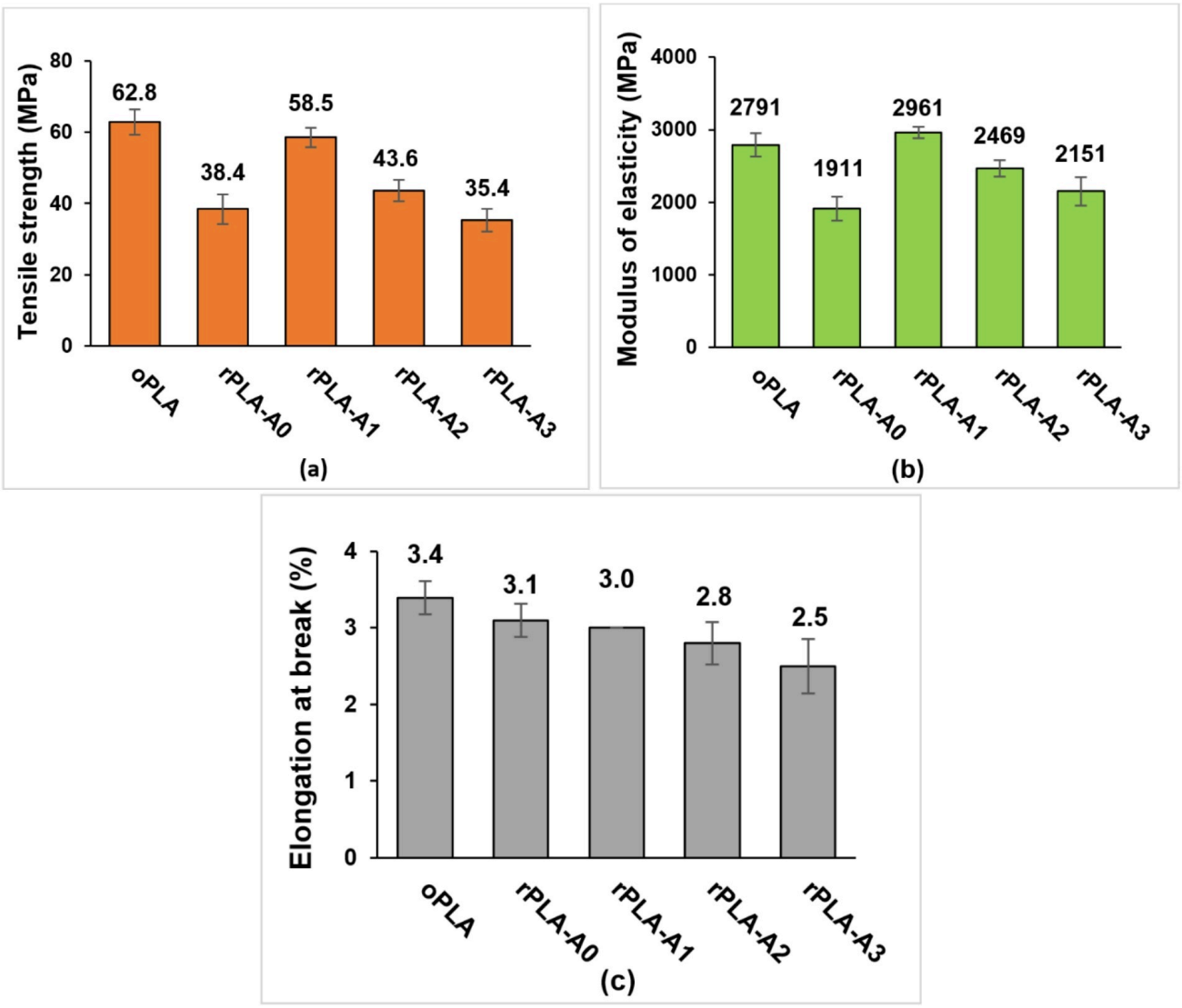

Figure 1

Tensile properties of oPLA and recycled PLA (rPLA) composites reinforced with varying agave fiber loadings: (a) tensile strength, (b) modulus of elasticity, and (c) elongation at break.

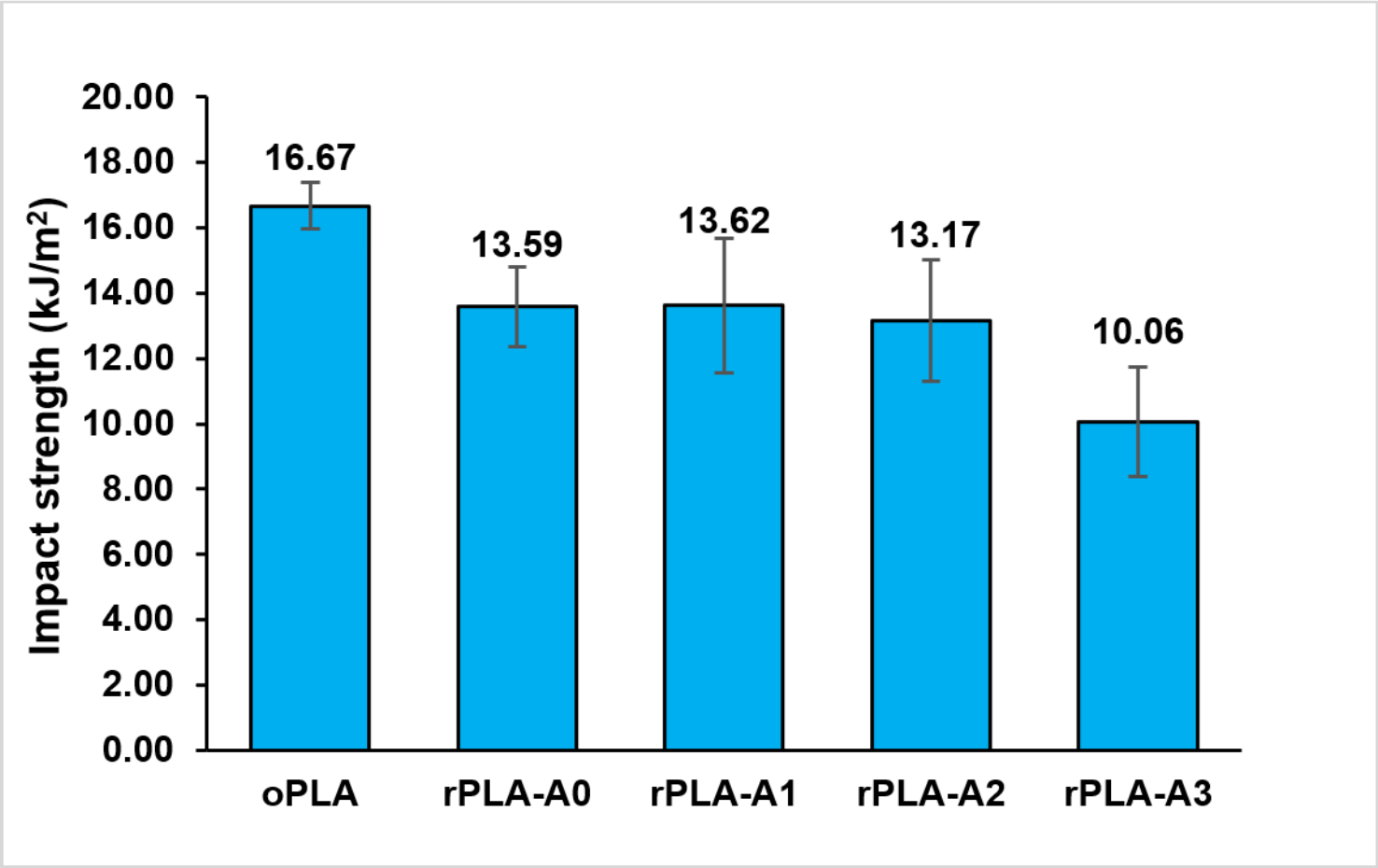

Figure 2

Impact strength of pristine PLA (oPLA), recycled PLA (rPLA-A0) and PLA/agave fiber composites (rPLA-A1, rPLA-A2, rPLA-A3)

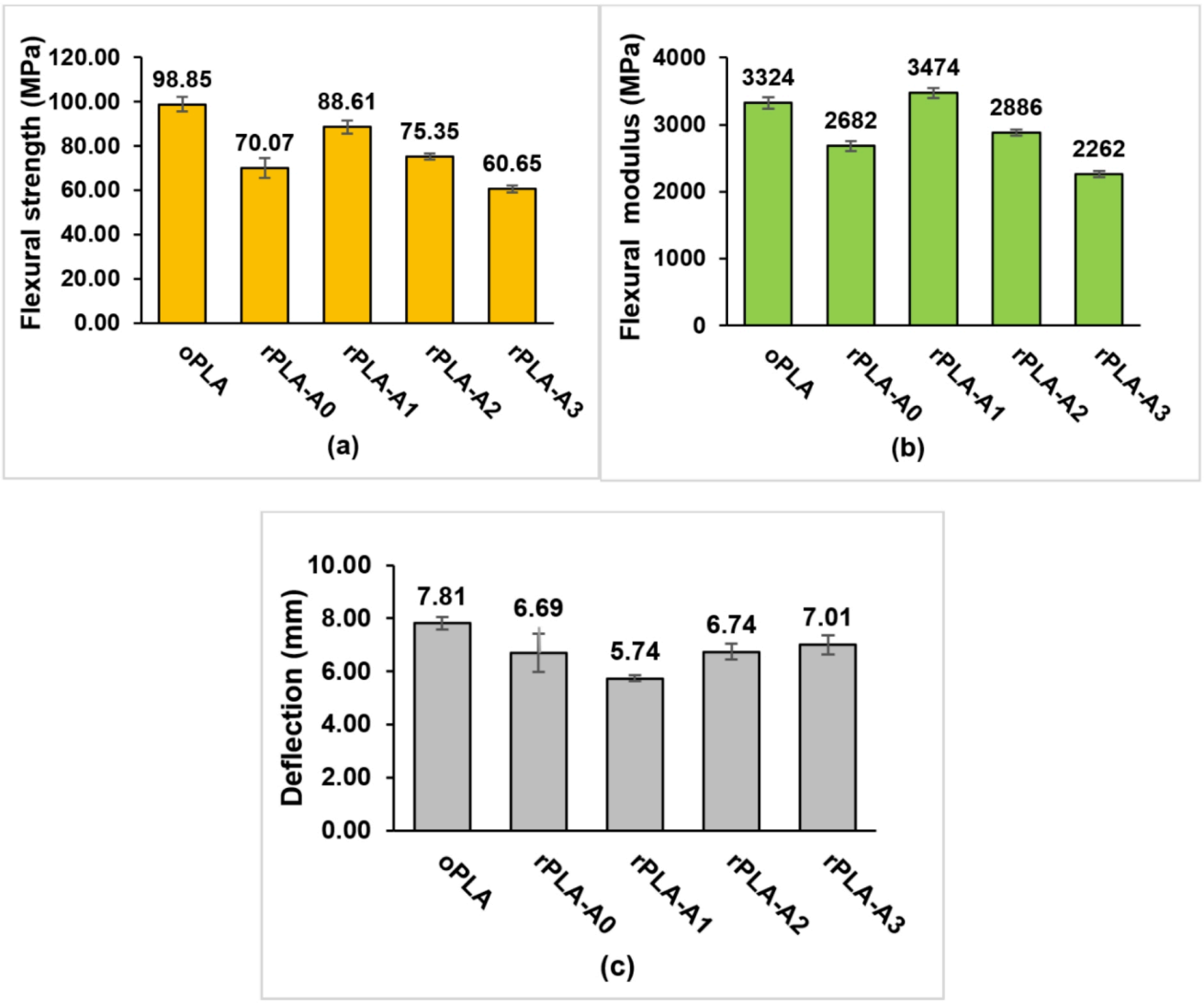

Figure 3

Flexural properties of PLA and recycled PLA (rPLA) composites reinforced with varying agave fiber loadings: (a) flexural strength, (b) flexural modulus, and (c) deflection at maximum bending.

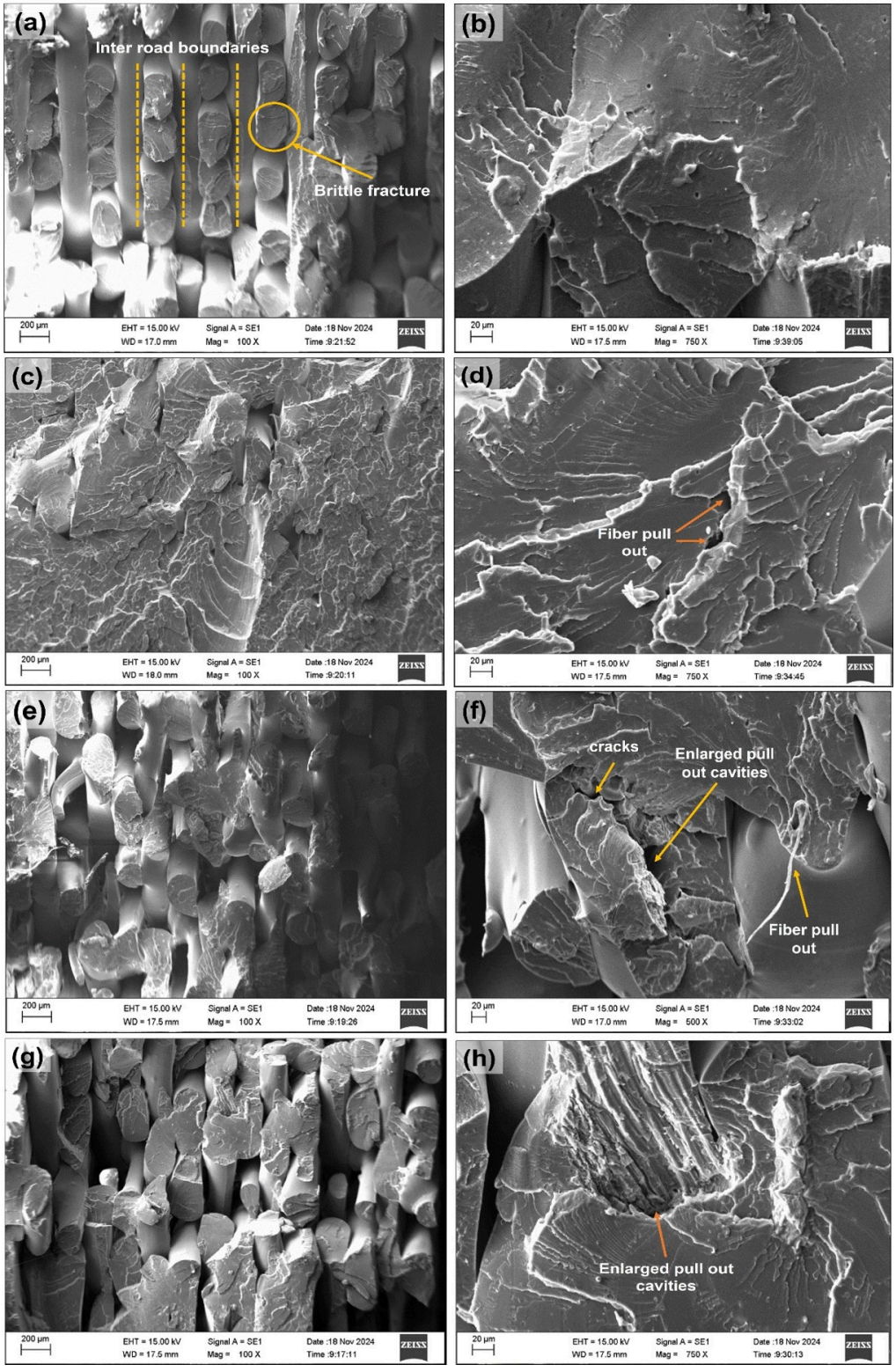

Figure 4

SEM micrographs of fracture surfaces of (a, b) recycled PLA (rPLA), (c, d) rPLA–A1 (1 wt.% agave fiber), (e, f) rPLA–A2 (2 wt.% agave fiber), and (g, h) rPLA–A3 (3 wt.% agave fiber) at low and high magnifications, respectively.

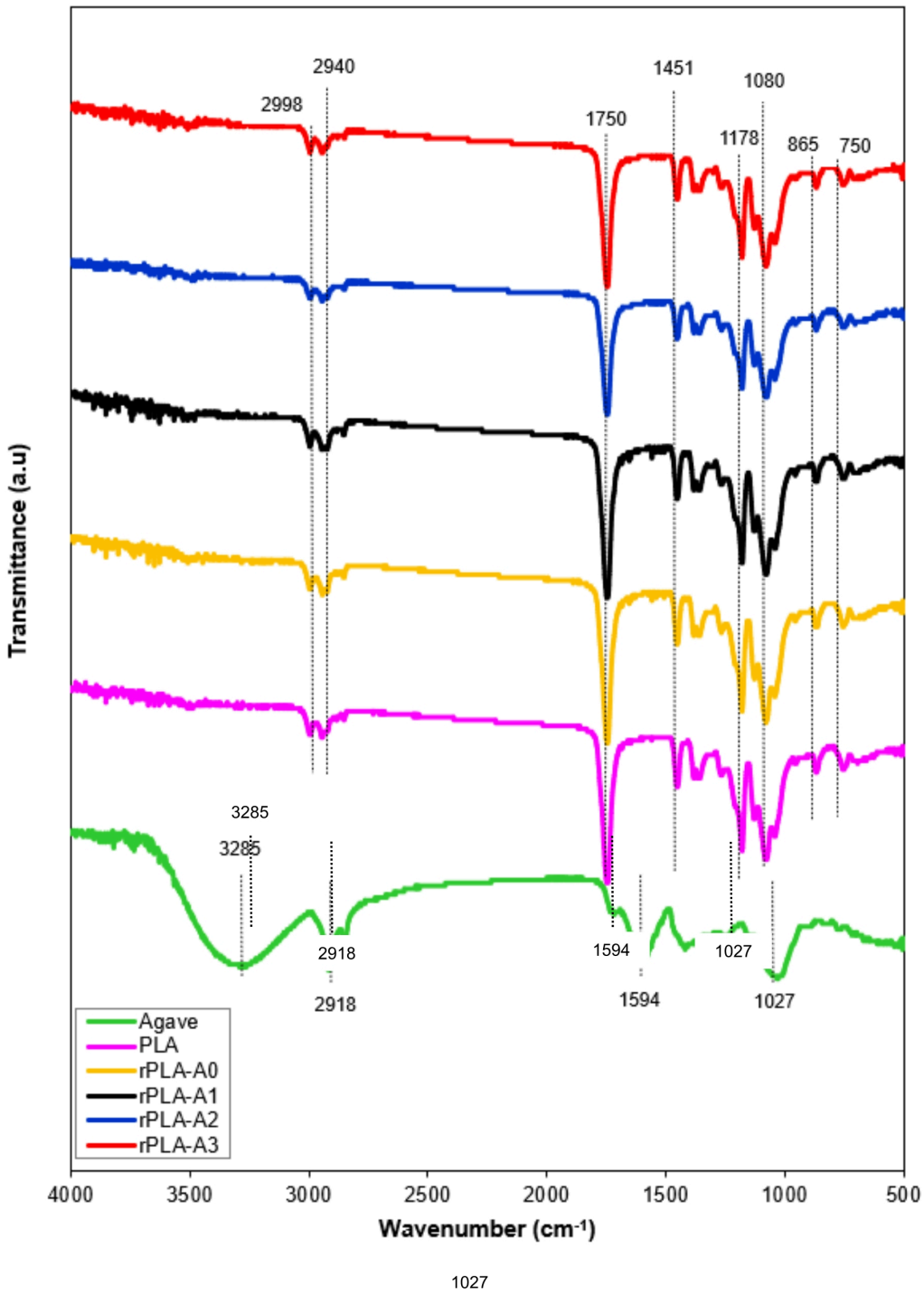

1027

Figure 5

FTIR spectra of raw agave fiber, pristine PLA, recycled PLA and rPLA-agave bio-composites.

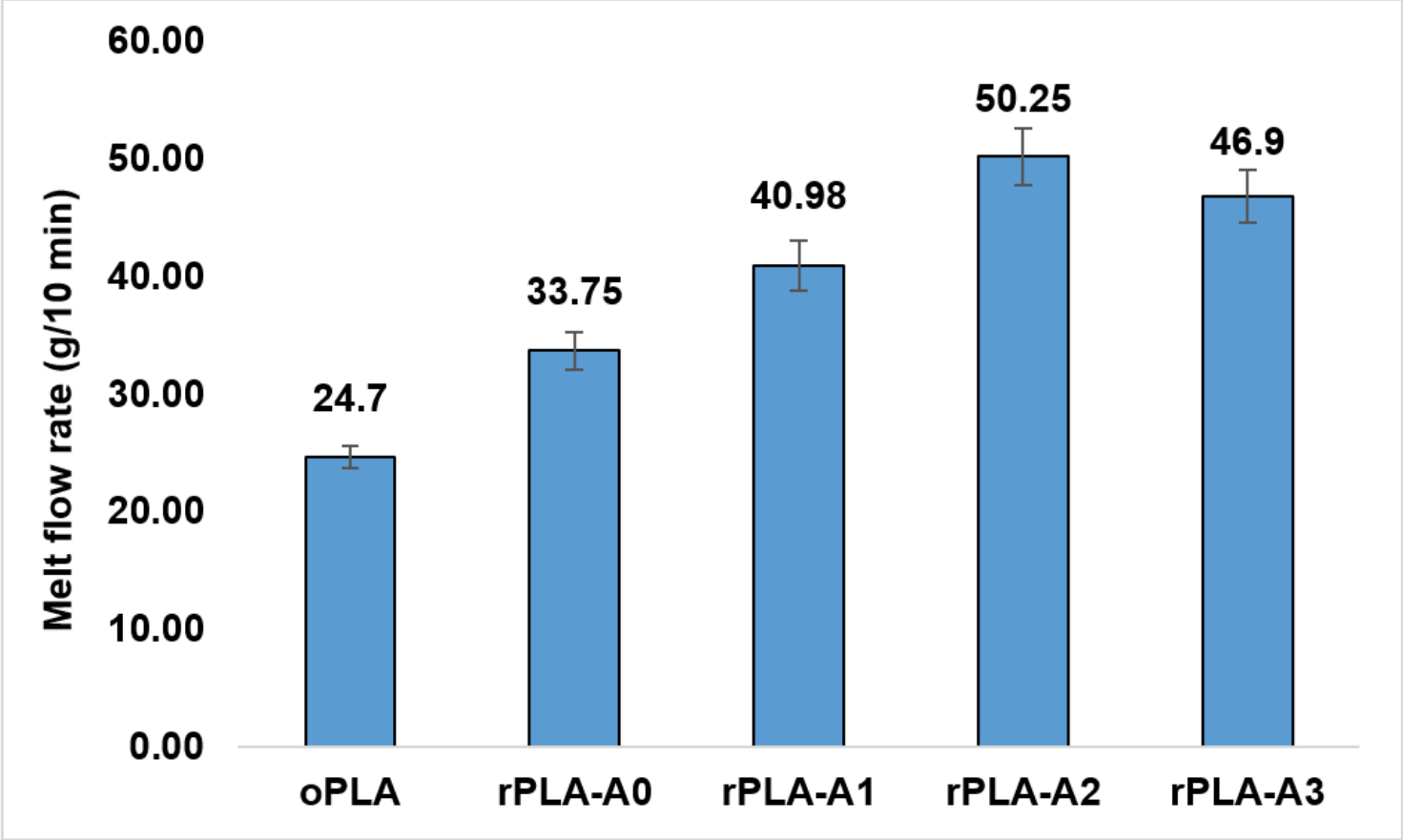

Figure 6

Melt Flow Rate (MFR) of pristine PLA, recycled PLA and its composites